

UCSF

UC San Francisco Previously Published Works

Title

Systematic identification of engineered methionines and oxaziridines for efficient, stable, and site-specific antibody bioconjugation

Permalink

<https://escholarship.org/uc/item/6ss6h5ps>

Journal

Proceedings of the National Academy of Sciences of the United States of America, 117(11)

ISSN

0027-8424

Authors

Elledge, Susanna K
Tran, Hai L
Christian, Alec H
et al.

Publication Date

2020-03-17

DOI

10.1073/pnas.1920561117

Peer reviewed



Systematic identification of engineered methionines and oxaziridines for efficient, stable, and site-specific antibody bioconjugation

Susanna K. Elledge^a, Hai L. Tran^a, Alec H. Christian^b, Veronica Steri^{c,d}, Byron Hann^{c,d}, F. Dean Toste^b, Christopher J. Chang^{b,e,f}, and James A. Wells^{a,g,1}

^aDepartment of Pharmaceutical Chemistry, University of California, San Francisco, CA 94158; ^bDepartment of Chemistry, University of California, Berkeley, CA 94720; ^cHelen Diller Family Comprehensive Cancer Center, University of California, San Francisco, CA 94158; ^dPreclinical Therapeutics Core, University of California, San Francisco, CA 94158; ^eDepartment of Molecular and Cell Biology, University of California, Berkeley, CA 94720; ^fHoward Hughes Medical Institute, University of California, Berkeley, CA 94720; and ^gDepartment of Cellular and Molecular Pharmacology, University of California, San Francisco, CA 94158

Contributed by James A. Wells, January 17, 2020 (sent for review November 25, 2019; reviewed by Peter S. Kim and Shohei Koide)

The field of chemical modification of proteins has been dominated by random modification of lysines or more site-specific labeling of cysteines, each with attendant challenges. Recently, we have developed oxaziridine chemistry for highly selective modification of methionine called redox-activated chemical tagging (ReACT) but have not broadly tested the molecular parameters for efficient and stable protein modification. Here we systematically scanned methionines throughout one of the most popular antibody scaffolds, trastuzumab, used for antibody engineering and drug conjugation. We tested the expression, reactivities, and stabilities of 123 single engineered methionines distributed over the surface of the antibody when reacted with oxaziridine. We found uniformly high expression for these mutants and excellent reaction efficiencies with a panel of oxaziridines. Remarkably, the stability to hydrolysis of the sulfimide varied more than 10-fold depending on temperature and the site of the engineered methionine. Interestingly, the most stable and reactive sites were those that were partially buried, presumably because of their reduced access to water. There was also a 10-fold variation in stability depending on the nature of the oxaziridine, which was determined to be inversely correlated with the electrophilic nature of the sulfimide. Importantly, the stabilities of the best analogs were sufficient to support their use as antibody drug conjugates and potent in a breast cancer mouse xenograft model over a month. These studies provide key parameters for broad application of ReACT for efficient, stable, and site-specific antibody and protein bioconjugation to native or engineered methionines.

chemical biology | bioconjugation | oxaziridine methionine chemistry | antibody drug conjugate | protein engineering

Chemical modification of natural amino acids in proteins has a long and storied history but largely is limited to modification of thiols and amines with various electrophiles (1). Recently, a methionine specific chemistry has been developed, called redox-activated chemical tagging (ReACT) (Fig. 1A) (2). The ReACT chemistry involves oxidation of methionine to form a sulfimide adduct with an oxaziridine molecule functionalized with an alkylzide to allow cargo attachment via click chemistry. Methionine is the second least abundant residue in proteins after tryptophan (3), making it a potentially ideal target for site-specific conjugation. Most methionine residues are buried and therefore inaccessible, making it an excellent candidate for bioengineered single-site chemical conjugation. However, the structural and chemical parameters for reaction of methionines in a folded protein with oxaziridines have not been systematically evaluated for protein bioconjugation.

Antibodies represent the most popular target for bioconjugations because they are among the most versatile tools in biology and medicine (4). Chemical bioconjugation has been instrumen-

tal in expanding the utility of monoclonal antibodies, as both probes and therapeutics, by facilitating covalent attachment of a variety of moieties such as fluorophores (5), metal chelators (6), and nucleic acids (7–9), as well as toxins in the form of antibody drug conjugates (ADCs) (10–13). ADCs can be an improvement over standard chemotherapy treatment by simultaneously increasing targeting efficiency and reducing off-target toxicity (14–17). There are currently five Food and Drug Administration (FDA)-approved ADCs and more than 100 clinical trials to develop new ADC therapies (14, 16).

Ideally, the chemical modification should be efficient, stable, reproducible, and site-selective for homogeneity (16). Researchers have typically targeted lysine or cysteine residues for chemical conjugation because of high reactivity and yield to form stable adducts via amide bonds with lysines or thioether linkages to cysteines (14–17). Three out of the five FDA-approved ADCs target lysines for conjugation (17). However, antibodies typically have about 40 surface exposed lysine residues per IgG that can result in more than 1 million

Significance

Site-specific chemical modification of proteins remains a critical need for bioconjugation. Here we explore the key parameters needed for efficient, selective, and stable modification of methionine using recently developed oxaziridine reagents, called ReACT. We systematically tested various oxaziridine compounds, and scanned accessible and buried sites in a therapeutic antibody for breast cancer to determine the chemical and structural parameters for most stable and efficient modification. We show these adducts are highly stable over days and can support the delivery of toxic payloads to regress tumors in animals. These studies on this important chemical modification expand our capability to site-specifically modify proteins and antibodies for many applications.

Author contributions: S.K.E., H.L.T., and J.A.W. designed research; S.K.E., H.L.T., and V.S. performed research; S.K.E., H.L.T., A.H.C., F.D.T., and C.J.C. contributed new reagents/analytic tools; S.K.E., H.L.T., A.H.C., V.S., B.H., and F.D.T. analyzed data; and S.K.E. and J.A.W. wrote the paper.

Reviewers: P.S.K., Stanford University School of Medicine; and S.K., New York University School of Medicine.

Published under the PNAS license.

Competing interest statement: S.K.E., H.L.T., J.A.W., and the Regents of the University of California have filed a patent application (US Provisional Patent Application UCSF073P) related to engineered methionine mutants on antibody scaffolds.

¹To whom correspondence may be addressed. Email: jim.wells@ucsf.edu.

This article contains supporting information online at <https://www.pnas.org/lookup/suppl/doi:10.1073/pnas.1920561117/-DCSupplemental>.

First published March 2, 2020.

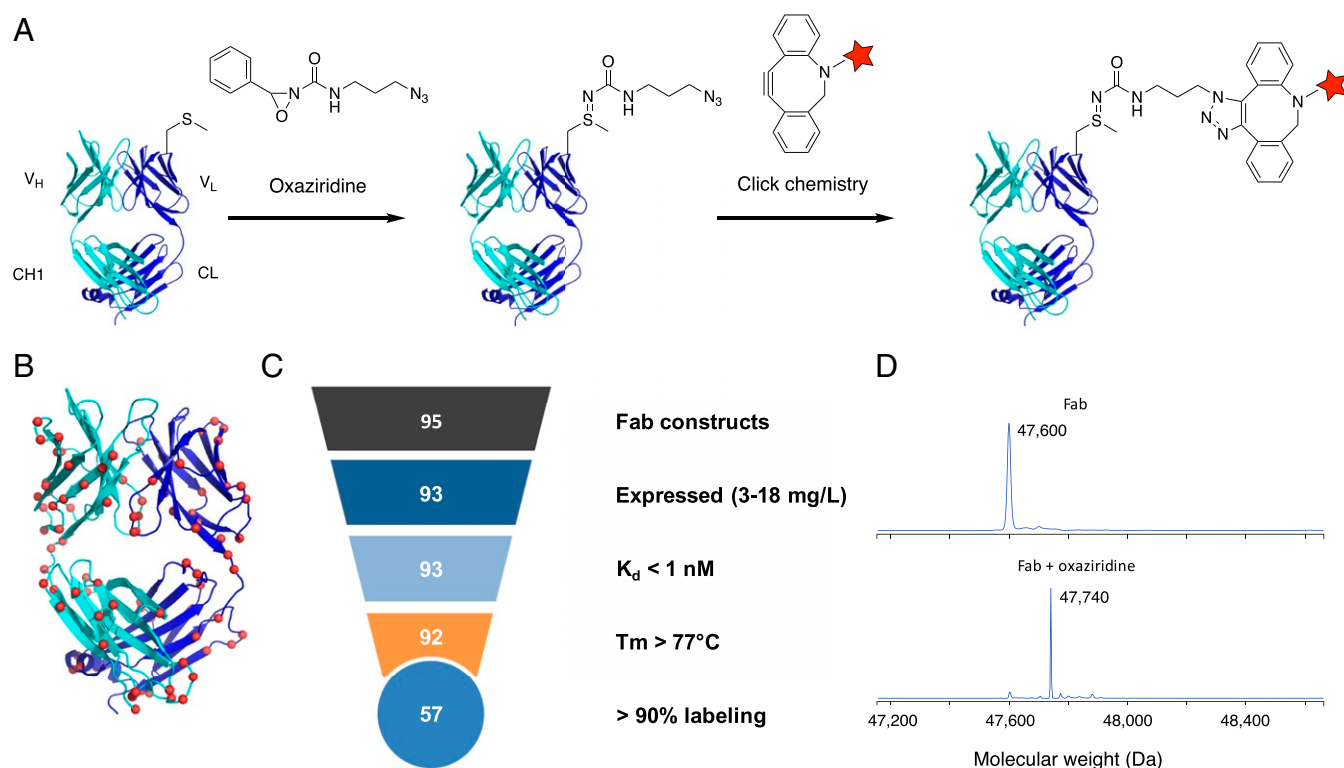


Fig. 1. Oxaziridine labeling of most accessible sites on model α GFP-Fab in the trastuzumab scaffold. (A) Scheme for oxaziridine labeling on trastuzumab Fab. The Fab light chain is shown in dark blue, and the heavy chain is shown in cyan. After conjugation with oxaziridine, different functionalities can be clicked on with a DBCO reagent. (B) The top 95 calculated accessible sites on the Fab scaffold are shown as red spheres. (C) Triage of the 95 most accessible mutants is shown. Each site was engineered to methionine on a model α GFP-Fab in the trastuzumab scaffold. Sites were then assessed for expression, affinity, structural stability, and labeling percentage. (D) Representative ESI mass spectra of one labeling reaction of α GFP Fab.Cmet with oxaziridine, shown by a mass shift of 140 (expected: 140).

different ADC species and drug antibody ratios (DARs) varying between 1 and 8 (16), which can lead to aggregation, immunogenicity, faster clearance rates, and differences in the pharmacodynamic properties of the conjugate (14, 18). Cysteine is becoming more commonly used as it is far less abundant than lysine and affords greater site-selectivity. However, this approach usually involves random reduction of the inter-chain disulfide bonds of the antibody that can still lead to heterogeneous mixtures (14, 19, 20). Recently, researchers have systematically introduced single cysteine residues into the therapeutic antibody, trastuzumab, to identify sites for stable and specific conjugation (21, 22). Other conjugation strategies are being developed such as enzymatic conjugation, glycan modification, and unnatural amino acid incorporation (14, 17). These strategies can result in homogenous conjugates but can be limited in terms of DAR and involve introducing scars, either by peptide motifs or altered natural glycosylation (17).

Here we methodically explore ReACT to determine how the methionine site and oxaziridine compound properties affect yield and stability in a folded protein, a therapeutic antibody. We systematically scanned 123 single methionine residues, which vary in accessibility in the trastuzumab scaffold, to identify sites and compounds for optimal conjugation yield and stability. We identified systematic factors that affect stability by more than 10-fold that we believe are portable to other antibodies and proteins. We found sites of high stability and produced potent ADCs with DARs of 2 or 4 that kill tumor cells *in vitro* and *in vivo* over a month. These studies show that the methionine oxaziridine reaction is a promising approach for site-specific, high yielding, and stable protein bioconjugations.

Results

High-Throughput Scan of the Top 95 Most Accessible Sites on the Trastuzumab Scaffold. We chose trastuzumab as the antibody scaffold of choice for our studies for a number of reasons. The trastuzumab framework is popular for humanization due to its high stability, high expression in mammalian cells, high developability, and broad use that is now utilized in parts of three different approved antibody drugs (trastuzumab, bevacizumab, and omalizumab) and the TDM-1 anti-Her2 ADC (ado-trastuzumab emtansine). Synthetic complementarity-determining region (CDR) libraries have been constructed on the trastuzumab scaffold (23) and used by the Recombinant Antibody Network for industrialized recombinant antibody generation to over 500 protein targets (24). The Fab arms in trastuzumab contain three methionines that are buried (*SI Appendix, Fig. S1*). Indeed previous studies from our group showed these buried methionines to be unreactive to ReACT, but when we attached a single Met to the C terminus of the light chain we found it could be labeled quantitatively with a simple oxaziridine reagent and conjugated with a fluorophore (2). While this site can be labeled quantitatively and could be useful for short-term *in vitro* studies, we found it becomes extensively (>80%) hydrolyzed over 3 d at 37 °C (*SI Appendix, Fig. S2*) and thus is not suitable for long-term studies or ADC development.

To expand the use of ReACT for antibody bioconjugations we sought to systematically determine how methionine mutation, site of labeling, and compound nature affect expression, labeling efficiency, binding affinity, and stability of the antibody (Fig. 1A). We first focused on exposed sites on a well-characterized α GFP antibody built on the trastuzumab scaffold as a model for ease of assay (24). We calculated the surface accessibility of

the methionine sulfur for all possible surface methionine substitutions. We mutated the top 95 most accessible sites to methionine (Fig. 1B and *SI Appendix*, Table S1) and expressed each individual mutant in the α GFP Fab without mutating the three intrinsic and unreactive buried methionines. Remarkably, of those 95 sites, 93 methionine mutants expressed with high yield in *Escherichia coli* (3 to 18 mg/L). All 93 retained high binding affinity for GFP after conjugation with oxaziridine and sulfo-DBCO-NH₂, and 92 of those retained high thermostability as measured by differential scanning fluorimetry. When tested for labeling with five equivalents of the oxaziridine reagent (oxaziridine 1) for 2 h, 57 mutants labeled to greater than 90% (Fig. 1C and *SI Appendix*, Fig. S3). This could potentially be improved with higher equivalents of oxaziridine. All mutants labeled stoichiometrically and specifically at the mutated methionine residue, as determined by whole protein mass spectrometry (Fig. 1D and *SI Appendix*, Table S1). These data suggest tremendous flexibility in generating site-specific methionine conjugations.

While these sites are likely useful for short-term studies such as immunofluorescence or other in vitro studies, we wanted to test their suitability for longer-term in vivo applications. Of the 57 highly labeled sites, we chose 12 representative sites to test conjugation stability as a function of location and temperature (Fig. 2A). The 12 candidate sites spanned both the heavy and light chains, as well as the variable and constant domains of the Fab arm. We incubated each methionine-oxaziridine conjugate at 4, 25, and 37 °C for 3 d and measured the remaining conjugate

by whole protein MS (Fig. 2B). We found a strong temperature dependence for hydrolysis from 4, 25, and 37 °C. There was considerable variation among the sites, but all sites had less than 60% remaining conjugate after 3 d at 37 °C. The product had a +16 mass shift consistent with hydrolysis of the sulfimide to a sulfoxide product, which has also been previously reported (25). Since ADCs can have circulation times up to weeks in the body, it is essential that the linkage is stable for an extended period at biological temperatures to retain ADC potency and to eliminate off-target toxicity due to free drug release. Although these stabilities are sufficient for the many in vitro uses for antibody conjugation, we sought to extend the stability of the antibody conjugate for ADCs.

Enhancing Stability of Oxaziridine Conjugates. We took two approaches to improve conjugation stability: 1) test different substituted oxaziridine analogs to improve linkage stability and 2) test more buried sites on the Fab scaffold that we hypothesized could better shield the sulfimide from hydrolysis. We obtained 15 different oxaziridine molecules with various functionalities appended to the urea group to determine if the resulting sulfimide bond could be further stabilized (Fig. 2C). We chose one representative site, LC.T20M, that showed moderate stability at 37 °C for oxaziridine 1. All compounds were conjugated to LC.T20M site on the model α GFP Fab, and stability of the sulfimide linkage was measured at 37 °C over 3 d. There was considerable variation in stability from 40 to 90% retained; nonetheless, two of oxaziridines (compounds 5 and 8) provided

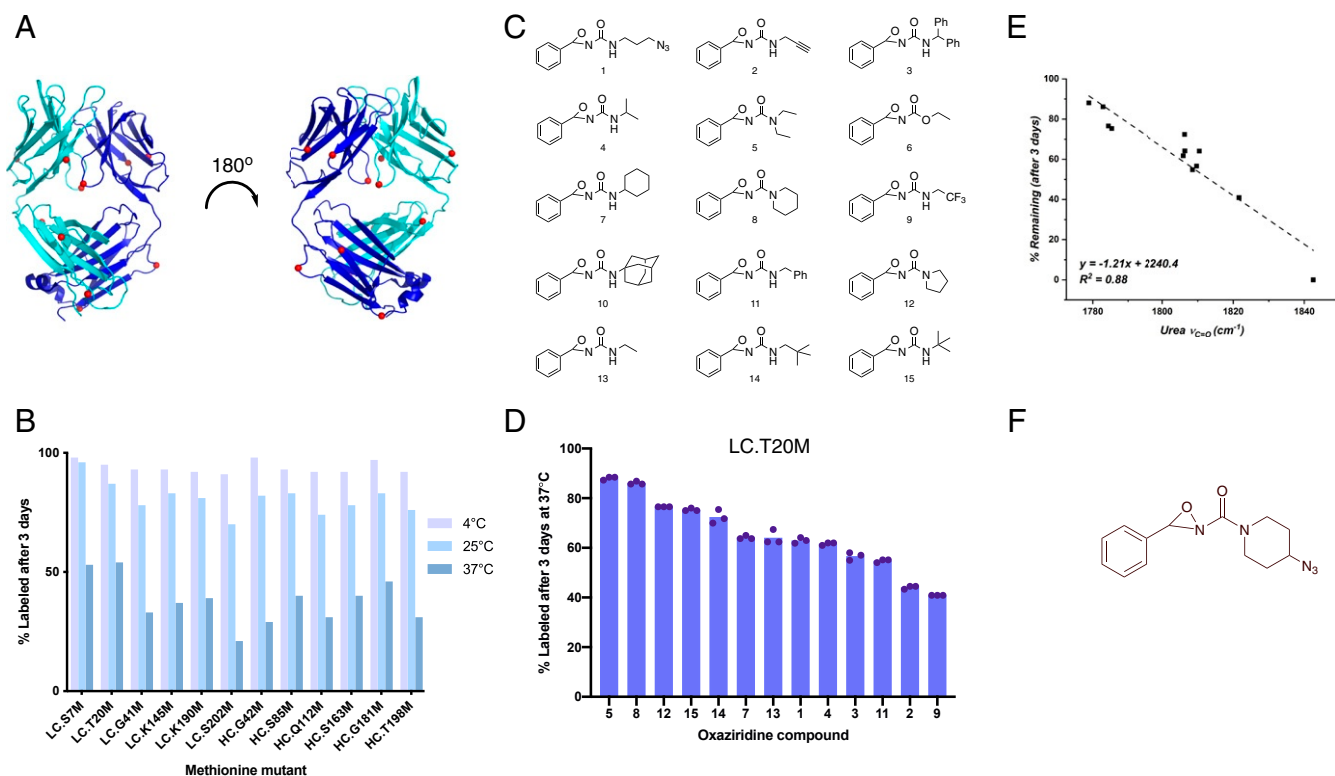


Fig. 2. Labeling and stability of top 12 accessible sites with different oxaziridine compounds. (A) Ribbon diagram of the trastuzumab Fab where the top 12 labeled sites (all >95% labeling yield) are shown as red spheres. (B) Stability of top 12 sites labeled with oxaziridine at 4, 25, and 37 °C over 3 d varies across sites and temperatures. All sites show a significant decrease in stability to hydrolysis at elevated temperatures. Each data point represents one measurement from one sample at that temperature. (C) Panel of oxaziridine compounds tested for stability. (D) Conjugate stability at site LC.T20M over 3 d at 37 °C when reacted with each oxaziridine. Oxaziridine 6 is not shown because it showed 0% conjugation stability after 3 d. Oxaziridine 10 is not shown because no initial labeling could be detected. Each bar height represents the average from three biological replicates. (E) Correlation of compound conjugate stability of LC.T20M and carbonyl stretching frequency ($\nu_{C=O}$). The more electron rich the substitution on the oxaziridine, the less electrophilic the sulfimide becomes, thus increasing conjugate stability on the protein. Each data point represents the mean of three individual samples. (F) The structure of the azide derivative of the piperidine-derived oxaziridine 8.

stability over 80% (Fig. 2D). In a recent parallel study, it was shown that conjugate stability to isolated methionine was related to the electron density around the carbonyl as measured by the carbonyl stretching frequency (25). Indeed, we found a strong inverse correlation between carbonyl stretching frequency and the measured stabilities on the Fab (Fig. 2E) as was also seen with isolated methionine. We synthesized a new azide containing oxaziridine derivative, based on the more stable piperidine-derived oxaziridine 8, to enable copper-free click chemistry for ADC conjugation (Fig. 2F).

We next investigated how lowering site accessibility may shield the resulting sulfimide linkage from hydrolysis. We knew that fully buried sites are unreactive and therefore chose 23 sites that had intermediate degrees of accessibility (Fig. 3A and *SI Appendix, Table S2*), most of which were located on structured β -sheet regions. Remarkably, 19 of the 23 single methionine substitutions at these partially buried sites expressed at high levels in *E. coli* (3 to 50 mg/L); 18 retained high affinity to GFP, and 17 retained high thermostability (Fig. 3B). These less accessible sites were also less reactive, and thus, we increased the labeling reaction to 20 equivalents of oxaziridine to better drive the reactivity. We found four mutants that had greater than 85% stability when labeled with the oxaziridine azide 8 and incubated at 37 °C for 3 d (Fig. 3B and C). There was a slight inverse correlation between site accessibility and long-term stability (Fig. 3D), but the lack of a strong correlation suggests that additional factors are partly responsible. Overall, we found the combination of probing different oxaziridine derivatives and different site accessibility produced highly stable conjugates that were candidates for ADC production.

We next incorporated these mutations into a trastuzumab Fab and tested the ADC conjugates for killing of breast cancer cell lines. However, we noticed that the wild-type trastuzumab

Fab labeled 25% with the oxaziridine reagent when reacted at 20 equivalents, which was a necessary concentration of oxaziridine to label the less accessible sites (*SI Appendix, Fig. S44*). We hypothesized this additional and undesirable labeling was due to labeling of the methionine at position HC.M107 in the CDR H3 of trastuzumab. Simply mutating HC.M107 to an unreactive leucine eliminated labeling at this site (*SI Appendix, Fig. S44*). The HC.M107L mutation did not affect binding to HER2 on SKBR-3 cells (*SI Appendix, Fig. S4B*).

We chose our two most stable sites, LC.R66M and LC.T74M, and incorporated methionine into the corresponding sites on trastuzumab α HER2 Fab antibody to use in cellular toxicity and serum stability assays. Both labeled to greater than 80% when reacted with 20 equivalents of oxaziridine-azide 8 (*SI Appendix, Table S2*). The two stable sites were individually converted to methionines on the trastuzumab Fab scaffold and then labeled with oxaziridine azide 8, followed by strain promoted click chemistry with DBCO-PEG4-valine-citrulline-MMAF to be used in a cellular toxicity assay. We chose to use the cathepsin B cleavable linker valine-citrulline for its improved effect over a noncleavable linker (data not shown). We picked the microtubule inhibitor MMAF as the toxic payload due to its previously characterized strong potency in ADC formats and improved solubility compared to MMAE (26). Both ADCs showed high potency in a HER2-positive breast cancer cell line, BT474-M1, compared to either trastuzumab alone or an α GFP Fab isotype control (Fig. 3E). The ADC conjugates were 10- to 100-fold more potent than the free MMAF reflecting their capacity as a drug chaperone. Interestingly, the ADC derived from the LC.R66M was about 10-fold less active than LC.T74M due to a modest loss in affinity when conjugated with drug (*SI Appendix, Fig. S5A*). Fortunately, upon conversion to a full IgG, the loss in affinity was greatly restored

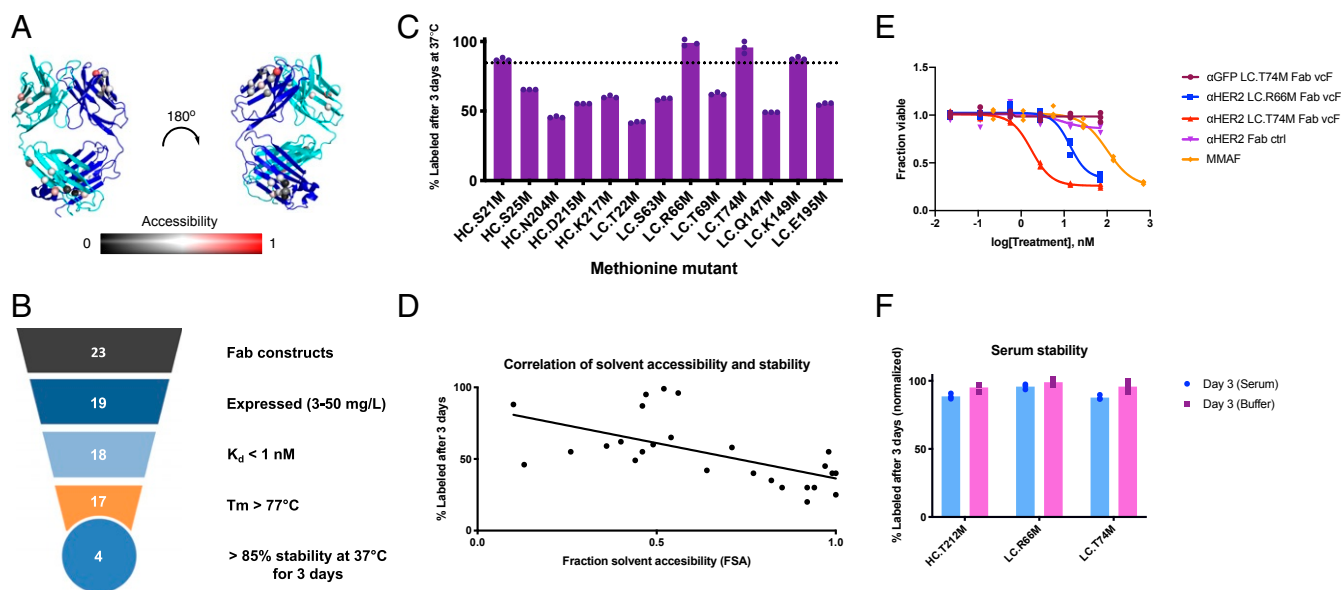


Fig. 3. Labeling, stability, and activity of partially buried sites on α GFP-Fab and Trastuzumab Fab. (A) Structure of the trastuzumab Fab showing 23 partially buried sites (spheres) chosen to mutate to methionine. Scale represents calculated relative fractional surface accessibility from 0 (black) to 1 (red). (B) Triage of the 23 individual mutants on the α GFP-Fab after testing expression, binding to GFP, structural stability, and oxaziridine conjugate stability for 3 d at 37 °C. (C) Conjugate stability of 14 sites after incubation at 37 °C for 3 d. The dotted line indicates 85% stability. Three biological replicate data points are shown. (D) Correlation between measured stability at 37 °C and calculated accessibility for the 23 partially buried sites. Linear regression analysis using GraphPad Prism was used to calculate the coefficient of determination ($R^2 = 0.32$) to determine correlation. (E) In vitro potency of two stable sites on trastuzumab Fab on the BT474-M1 breast cancer cell line. An α GFP conjugated Fab was included as an isotype control. Three biological replicate data points are shown. (F) Stability measured in human serum for oxaziridine conjugates at the three top stable sites over 3 d at 37 °C compared to stability measured in buffer. Three biological replicate data points are shown.

due to the higher avidity of the IgG and much lower off-rates (*SI Appendix, Fig. S5B*). Both sites were also tested for their stability in human serum and showed similar levels compared to their stability measured in buffer (Fig. 3*F*). Thus, the two sites in the Fab arms are promising candidates for ADC formation.

Labeling and Stability at Homologous Sites on the Fc Domain. To explore more flexibility in labeling sites for methionine antibody conjugates, we probed for suitable labeling sites on the Fc domain of the IgG. We found there are two endogenous methionines on the Fc (HC.M252 and HC.M428) that are surface exposed and one of which readily reacts with the oxaziridine azide 8 (Fig. 4*A* and *SI Appendix, Fig. S6A*). Also, it is known that these methionines sit directly at the FcRn binding site and that even oxidation at these sites can disrupt FcRn binding (27). In fact, labeling these methionines with oxaziridine ablated FcRn binding, detected by biolayer interferometry (*SI Appendix, Fig. S6B*). Thus, we scrubbed these methionines by mutation to leucine as above and found these had little to no effect on overall protein stability or FcRn binding ability (*SI Appendix, Fig. S6C*). We also incorporated an N297G mutation to prevent glycosylation of the Fc to simplify our mass spectrometry analysis. We then used this Fc mutant as our template to search for more stable methionine conjugation sites.

To simplify our quest for new methionine sites in the Fc we took advantage of the high structural similarity among the four Ig domains between the Fc (CH2-CH3) and Fab arms (V and CH1). We used PyMol to align the five most stable conjugation sites from the Fab arm studies above to sites in the Fc domain (Fig. 4*A* and *SI Appendix, Table S3*). An example alignment is shown between LC.K149 and HC.E382 (Fig. 4*B*). We introduced single methionine mutants into these sites in the native methionine-scrubbed Fc, expressed the variants in Expi293 mammalian cells, and tested them for their labeling efficiency and stability. Interestingly, two of the engineered sites (HC.T307M and HC.T437M) did not label at all and thus could not be tested for their stability. The other three sites labeled to over 50%, and site HC.V262M showed greater than 80% labeling efficiency with virtually no hydrolysis after a 3 d incubation at 37 °C (Fig. 4*C*).

Functional Activity of Methionine Oxaziridine ADCs on Breast Cancer Cell Lines and In Vivo Efficacy in a Breast Cancer Xenograft Model. We then tested how each of the three stable sites (LC.R66M, LC.T74M, and HC.V262M) performed as ADCs in an IgG format on HER2-positive breast cancer cell lines (Fig. 5*A* and *B*). On both SKBR-3 and BT474-M1 cell lines, all three sites were almost equally effective at reducing cell growth ($IC_{50} \sim 100$ to 1,000 pM). All three were 20- to 50-fold more potent than trastuzumab alone and trastuzumab with free MMAF (*SI Appendix, Fig. S7 A and B*). When compared to one of the previously reported optimal engineered cysteine sites, LC.V205C (22), we saw comparable cell killing to the LC.T74M site (Fig. 5*C*). We also saw improved efficacy of LC.T74M ADC compared to T-DM1 in the BT474-M1 cell line (*SI Appendix, Fig. S7A*) and similar efficacy to T-DM1 in the SKBR-3 cell line (*SI Appendix, Fig. S7B*). We also tested how these conjugates performed by size exclusion chromatography (SEC) as a test for antibody aggregates and a proxy for good pharmacokinetics. ADCs produced at sites LC.T74M and HC.V262M showed a single symmetrical elution peak comparable to trastuzumab, while site LC.R66M formed three broad peaks (*SI Appendix, Fig. S8*). Thus, we decided not to use site LC.R66M in vivo. We also discovered that after reintroducing the wild-type N297 residue and corresponding glycosylation, we were not able to label site HC.V262M, suggesting the glycosylation blocks labeling (*SI Appendix, Fig. S9*). Therefore, we nominated LC.T74M as our lead candidate for in vivo studies. We conjugated the LC.T74M trastuzumab IgG to the valine-citrulline cleavable MMAF with an average DAR of 1.9 (*SI Appendix, Fig. S10*) and performed a dose–response study in a mouse xenograft BT474-M1 breast cancer model (Fig. 5*D*). We saw dose–response efficacy and with the highest dose of 6 mg/kg saw inhibition of tumor growth compared to PBS control across 5 wk. All mice maintained healthy body weights during the study (*SI Appendix, Fig. S11*).

With these promising data, we sought to increase our efficacy by creating a DAR of four ADC with our Met sites. Ideally, we wanted not only a second site with high stability, but also a site spatially apart from the LC.T74M site to reduce the steric hindrance and potential for hydrophobic MMAF interactions between sites. Thus, we chose the partially buried stable site HC.S21M, which is almost directly opposite of the LC.T74M.

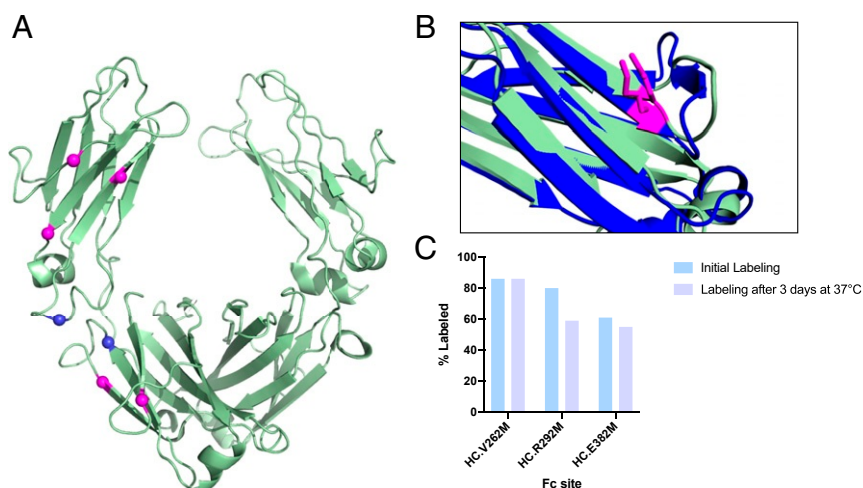


Fig. 4. Labeling, stability, and activity of homologous Fc sites. (A) Structure of IgG1 Fc domain (PDB ID 1H3X) showing five sites chosen to individually mutate to methionine (dark purple). The two endogenous methionines are shown in magenta. (B) Example alignment of part of the Fc domain with part of the Fab light chain to show the structural homology between site LC.K149 and HC.E383. (C) Stability and labeling measurements for three top sites on the Fc region. Two sites (HC.T307M and HC.T437M) are not shown because they did not produce viable conjugates with oxaziridine. Each data point represents a stability measurement from a single sample.

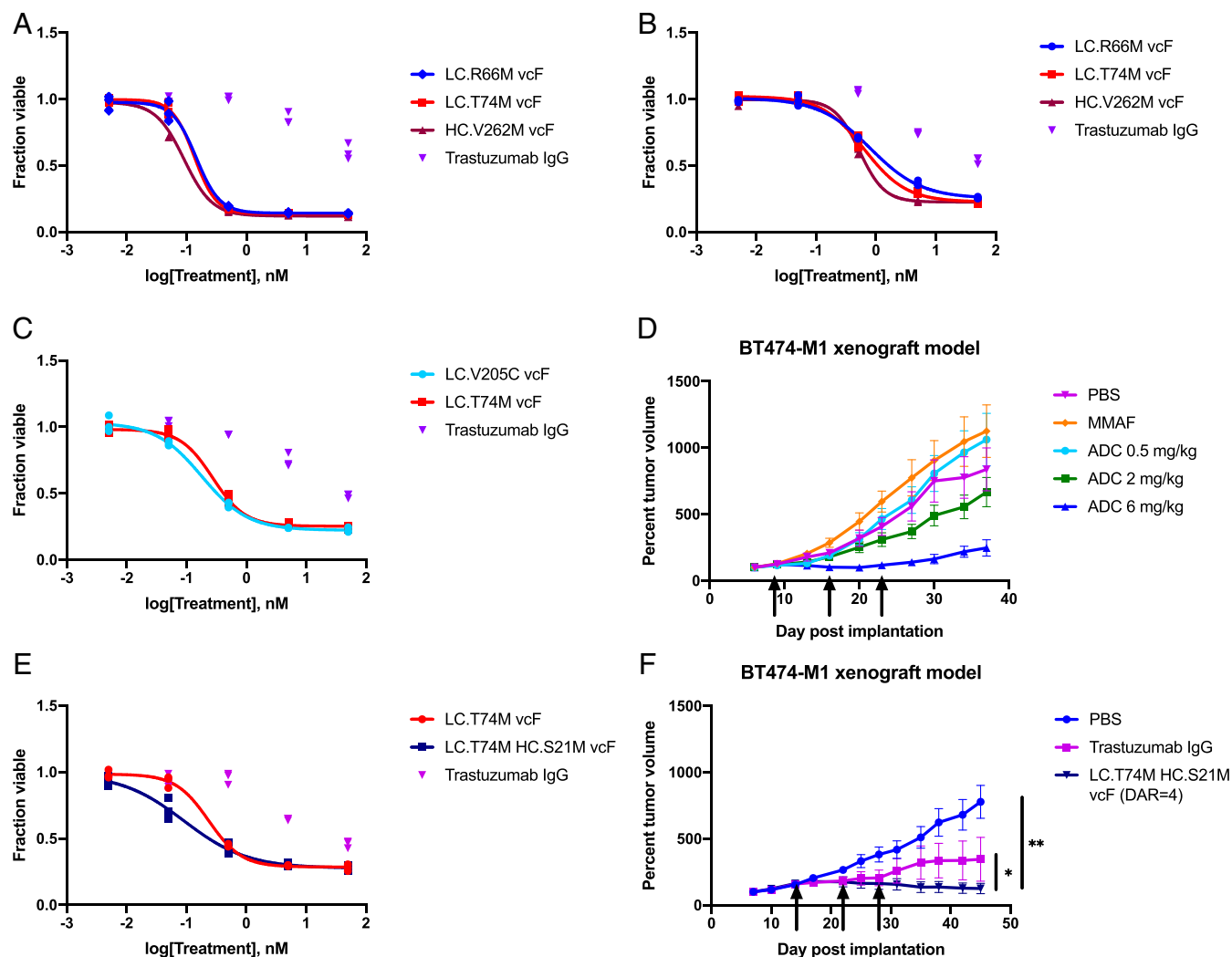


Fig. 5. In vitro and in vivo potencies of IgG-based ADCs in a breast cancer model. (A and B) In vitro potency of three sites (LC.R66M, LC.T74M, and HC.V262M) on two HER2-positive breast cancer cell lines, SKBR-3 (A) and BT474-M1 (B) against Trastuzumab unlabeled IgG control. Three biological replicate data points are shown. Trastuzumab unlabeled control is shown as individual points because of an insufficient plateau for curve fitting. (C) Comparison of site LC.T74M and stable cysteine site LC.V205C. (D) In vivo potency of site LC.T74M ADC in a breast cancer xenograft model in nude female mice, demonstrating clear dose response of the ADC. Arrows show intravenous administration schemes of PBS, MMAF, and ADCs. Lines indicate the average for each group, and error bars represent the SEM. (E) In vitro potency of DAR of two and DAR of four ADCs on the BT474-M1 cell line. Increasing to a DAR of four decreases the IC50 of the ADC from 0.24 nM (DAR = 2; red) to 0.091 nM (DAR = 4; dark blue). (F) In vivo potency of the DAR of four ADC with sites LC.T74M and HC.S21M in a BT474-M1 xenograft model in nude female mice (PBS, $n = 7$; Herceptin IgG, $n = 8$; ADC DAR of four, $n = 7$). Arrows show intravenous administration schemes of trastuzumab (10 mg/kg) and ADC (10 mg/kg). Lines indicate the average for each group, and error bars represent the SEM. $P = 0.0096$ (PBS:DAR4), $P = 0.0221$ (Trastuzumab:DAR4). * $P < 0.0332$, ** $P < 0.0021$ (one-way ANOVA test.)

After incorporation of both methionines into the HER2 IgG, we were able to obtain 80% labeling of the HC.S21M site with oxaziridine-azide 8 at 20 equivalents over 30 min. Using the double mutant we were able to obtain significant labeling of both sites with DBCO-PEG4-valcitic-MMAF with an average DAR of 3.6 (SI Appendix, Fig. S12). We evaluated the conjugate by SEC and saw a monodispersed peak, suggesting there were no aggregates (SI Appendix, Fig. S13). The DAR of 4 derivative showed an increase in in vitro efficacy on the BT474-M1 cell line compared to DAR of 2 derivative from the LC.T74M IgG (Fig. 5E). There was a slight decrease in cell binding with the DAR of 4 ADC compared to DAR of 2 ADC (SI Appendix, Fig. S14), possibly due to the increase in hydrophobicity. We then tested our DAR of 4 ADC (10 mg/kg) in the BT474-M1 xenograft model and saw efficacy in reducing tumor growth over 5 wk (Fig. 5F). The efficacy was greater than Trastuzumab IgG control (10 mg/kg), showing the use of these sites in an ADC

model. Healthy body weights were maintained for all mice except one mouse in the DAR of 4 treatment group (SI Appendix, Fig. S15). These data show the proof of concept application of using these engineered sites in ADCs and the potential for this method in future stable protein bioconjugation applications.

Discussion

We lay out a systematic and general approach for identifying efficient, stoichiometric, and stable methionine labeling sites for antibodies using ReACT that preserves antibody function and stability for stable protein bioconjugations such as ADCs. We explored a number of variables and addressed potential pitfalls to find optimal labeling sites. Surprisingly, almost all of the single methionine mutants were tolerated in the context of the trastuzumab scaffold. Of the 95 highly accessible methionine sites, 93 were expressed at wild-type levels, and 92 retained a T_m greater than 77 °C. Even for the 23 partially buried sites,

19 were expressed at wild-type levels, and 17 maintained a high T_m. We did not detect methionine oxidation for the purified recombinant antibodies expressed either as Fabs in *E. coli* or as IgGs expressed from mammalian cells. This obviated the need to chemically reduce prior to conjugation with oxaziridine. This is a substantial advantage to cysteine labeling, which typically requires reduction and reoxidation prior to thiol conjugation. The conjugation to the oxaziridine was done rapidly (30 min at 5- to 30-fold excess) at room temperature in aqueous conditions and consistently produced high yields of the bioconjugate. For example, of the 92 accessible methionine sites expressed, 57 were labeled over 90%. Even for the 23 expressible partially buried methionine sites, 11 were labeled to over 80%.

One can tolerate, manage, or exploit endogenous methionines for antibody conjugations. In our α GFP trastuzumab Fab, there are three buried methionines. We found them to be unreactive and thus preserved them throughout our experiments. Once we switched to the wild-type trastuzumab, there was a reactive methionine in CDR H3, but it was benignly replaced with a leucine and did not affect the affinity of the antibody. Moreover, methionines are routinely mutated out of CDRs in therapeutic antibodies to avoid oxidation upon long-term storage or treatment (28). We also identified two endogenous methionines in the Fc, and these were readily mutated to leucine without significant impact on expression or binding. In some cases, methionine sites have been mutated to nonoxidatively sensitive residues to extend antibody half-life and improve FcRn binding (29).

We found the initial oxaziridine compound did not have the desired stability for long-term studies, but structure–activity analysis identified compounds with significantly improved stability to hydrolysis. The stability tracked with the electron density surrounding the carbonyl as found in parallel studies on isolated methionine (25). We believe these compounds (especially oxaziridine azide 8) will find general utility for ReACT applications for other protein bioconjugations. We found significant variation in stability depending on the site of modification. There is an inverse trend between accessibility and site stability. We expect this may be because the sulfimide is shielded from water and hindered from being hydrolyzed. The hydrolysis reaction of the sulfimide is expected to go through a tetrasubstituted intermediate (30), and neighboring sites will likely impact the stability of this intermediate based on the chemical environment. Further mechanistic and computational work may help to further dissect these factors. Interestingly, the stability, and therefore therapeutic effectivity, of cysteine conjugates also varies depending on the conjugation sites (22, 31).

We believe site-specific modification of methionine by ReACT has great potential for antibody and protein bioconjugations. The expression of the methionine mutants is robust, and multiple methionines can easily be introduced. The conjugation procedure is rapid and simple and does not require prereduction. There is good flexibility with site selection, and the resulting linkage can be stable at biological temperatures. The sites described here will provide candidates for other antibody scaffolds. In fact, the discovery of the stable Fc site did not require a complete methionine surface scan, but rather simple homology modeling was sufficient to identify a stable site. Additionally, these sites may be useful for other methionine-specific conjugations that have recently been developed and could be applied to antibodies (32).

Site-specific methionine labeling by ReACT offers more homogeneity of modification compared to lysine and cysteine modification. It produced highly stable conjugates and robust ADC activity in a BT474-M1 mouse xenograft model. While there is still work to do to validate their clinical use, we believe this modification will be useful for many other antibody and protein bioconjugation applications such as for fluorescence, affinity

labels, DNA barcoding, and protein–protein bioconjugation. The general parameters studied and optimized here will expand the use of ReACT bioconjugation on many other biomolecules.

Materials and Methods

Selection of Accessible Conjugation Sites. To estimate the relative solvent accessibility (RSA) of engineered methionines on a Fab, a computational methionine scan was performed with MODELLER using Protein Data Bank (PDB) structure 1FVE as a template (33). MODELLER generates homology models for comparative structure analysis by satisfaction of spatial restraints (34). Single methionine mutations were systematically modeled across the entire structure of the Fab including an additional model with a methionine appended at the end of the light chain for a total of 439 individual models generated. The solvent accessible surface area (SASA) of the engineered methionine sulfur atom was determined using the “get_area” function (dot_solvent = 1, dot_density = 4, solvent_radius = 1.4) in PyMol. Due to the stochasticity of the S-methyl group placement, the group was removed prior to SASA calculations and was found to reduce variability. The RSA was calculated by taking the SASA values and dividing by the maximum SASA value observed in the set. Positions were rank ordered, and the top 95 sites with the highest RSA (excluding CDR positions, prolines, and cysteines) were selected for bioconjugation.

Preparation and Characterization of Fab and IgG Antibodies. All methionine mutants were made using QuikChange to introduce single codon mutations onto Fab or IgG. Fabs were expressed and purified by an optimized autoinduction protocol previously described (24). In brief, C43 (DE3) Pro + *E. coli* containing expression plasmids were grown in TB autoinduction media at 37 °C for 6 h, then cooled to 30 °C for 16 to 18 h. For IgG expression, the engineered methionine IgGs were expressed and purified from Expi293 BirA cells according to established protocol from the manufacturer. Briefly, 30 μ g of pFUSE (InvivoGen) vector was transiently transfected into 75 million Expi293 BirA cells using the Expifectamine kit. Enhancer was added 20 h after transfection. Cells were incubated for a total of 6 d at 37 °C in a 5% CO₂ environment before the supernatants were harvested by centrifugation. Both Fabs and IgGs were purified by Protein A affinity chromatography. Purity and integrity was assessed by SDS/PAGE and intact protein mass spectrometry.

Synthesis of Compounds. All oxaziridine compounds were previously synthesized and reported in Christian et al. (25). Synthesis of the azide-piperidine oxaziridine (oxaziridine azide 8) can be found in *SI Appendix, SI Methods*.

Conjugation of Engineered Methionine Fabs and IgGs with Oxaziridine and DBCO-PEG4-valcit-MMAF. For Fab ADCs, endotoxins were removed prior to conjugation using Pierce endotoxin removal kits (Thermo Fisher Scientific). For conjugation, Fabs were incubated at 50 μ M with 15 molar equivalents of compound 8 azide oxaziridine for 30 min at room temperature in PBS. For IgGs, IgGs were incubated at 10 μ M with 20 molar equivalents of compound 8 azide oxaziridine per methionine for 1 h at room temperature in PBS. For both, the reaction was quenched by the addition of methionine, and antibody was buffer exchanged into PBS using a 0.5-mL Zeba 7-kDa desalting column (Thermo Fisher Scientific). Then 5 molar equivalents of DBCO-PEG4-valcit-MMAF (Levena Biosciences) were added, and the click reaction proceeded overnight at room temperature. The conjugate was desalted twice using two 0.5-mL Zeba 7-kDa columns to remove excess unconjugated drug. Full conjugation was monitored by intact protein mass spectrometry using a Xevo G2-XS Mass Spectrometer (Waters).

Stability Measurements of Oxaziridine Labeled Fabs in PBS and Serum. Fabs were labeled as previously described, placed in either buffer or human AB serum (Valley Biomedical), and incubated at 37 °C. PBS samples were measured directly by intact protein mass spectrometry. Serum samples were able to be purified with an Ni-NTA column due to the presence of a His-tag on the Fab. The sample was then consequently measured by intact protein mass spectrometry to determine proportion of labeled Fab.

Conjugation of Engineered Cysteine ADCs for Comparison. Engineered cysteine conjugation was performed as previously reported (35). In brief, after purification of the LC.V205C mutant α HER2 IgG (see IgG expression), the IgG (10 μ M) was buffer exchanged into 50 mM Tris-HCl, pH 7.5, 2 mM EDTA. DTT was added at 40-fold molar excess and incubated at room temperature for 16 h. Desalting into PBS proceeded with 0.5-mL Zeba 7-kDa columns. DHAA was added in 15-fold molar excess to reoxidize the interchain disulfides for 3 h at room temperature. Maleimide-valcit-MMAF (BOC Sciences)

was added at threefold molar excess, and conjugation was monitored by mass spectrometry. Excess drug was removed by two 0.5-mL Zeba 7-kDa desalting columns.

Cell Culture of HER2-Positive Breast Cancer Cells. The BT474-M1 cell line was provided by the Preclinical Therapeutics Core at the University of California, San Francisco (UCSF), Helen Diller Cancer Center. These cells were maintained in DMEM media supplemented 10% FBS and 1X Pen/Strep. The SKBR-3 cells were purchased from the UCSF Cell Culture Facility. They were maintained in McCoy 5a media supplemented with 10% FBS and 1X Pen/Strep. Cell line identities were authenticated by morphological inspection. The SKBR-3 cell line identity was validated by UCSF Cell Culture Facility. Symptoms for *mycoplasma* contamination were not observed, and thus, no test for *mycoplasma* contamination was performed. All cell lines that were received as gifts were previously authenticated.

ADC Cell Killing Assay In Vitro. ADC cell killing assays were performed using an MTT modified assay to measure cell viability. In brief, 10,000 BT474-M1 or SKBR-3 cells were plated in each well of a 96-well plate on day 0. On day 1, Fab/IgG was added in a 10-fold dilution series. Cells were incubated for 120 h at 37 °C under 5% CO₂. On day 6, 40 μL of 2.5 mg/mL of Thiazolyl Blue Tetrazolium Bromide (Sigma Aldrich) was added to each well and incubated at 37 °C under 5% CO₂ for 4 h. Following, 100 μL of 10% SDS 0.01M HCl was added to lyse the cells to release the MTT product. After 4 h, absorbance at 600 nm was quantified using an Infinite M200 PRO-plate reader (Tecan). Data points were plotted using GraphPad Prism (version 8.2), and curves were generated by using nonlinear regression with Sigmoidal 4PL parameters.

ADC Study in Mouse Xenograft Model In Vivo. The xenograft was performed with 6- to 8-wk-old nude female mice (NCR, nu/nu) purchased from Taconic Labs ($n = 3$ per group for the dose response, $n = 8$ for the DAR = 4 study). Prior to tumor cell engraftment, mice were implanted s.c. with Estradiol pellet (0.36 mg, 60 d release; Innovative Research). BT474-M1 xenografts were then established by bilateral subcutaneous injection into the right and left flanks of mice with BT474-M1 tumor cells (5×10^6 cells in 100 μL of serum

free medium mixed 1:1 with Matrigel). When BT474-M1 xenografts reached average volume of 200 mm³ (measured as width × width × length × 0.52), mice were dosed intravenously weekly for 3 wk with PBS, drug alone (equimolar conjugated drug), and ADCs. Tumor size and body weight were monitored biweekly for 5 wk total. Data were plotted in GraphPad Prism, and SEM for the six tumors across three mice in each group was determined for the first study. For the second study, data were plotted and SEM was determined for seven mice in the PBS group, eight mice in the Trastuzumab control group, and seven mice in the DAR of 4 ADC group (one mouse is not shown due to early sacrifice due to low body weight), and eight tumors across eight mice in the second study. All experiments were performed in accordance with relevant guidelines and regulations and in full accordance with UCSF Institutional Animal Care and Use Committee. Statistical analysis was performed using a one-way ANOVA test in GraphPad Prism.

Materials and Correspondence

Correspondence and material requests should be addressed to J.A.W. All data supporting the results are available upon request.

ACKNOWLEDGMENTS. We thank the members of the Wells laboratory and AntibioMe for helpful discussions. We thank M. Hornsby for the αGFP Fab expression vector, A. Weeks for the αHER2 Fab expression vector, A. Cotton for the V205C mutant vector, and J. Zhou for input on the cell viability assay. We thank M. Moasser for the generous gift of T-DM1. J.A.W. thanks The Chan Zuckerberg Initiative and Biohub Investigator Program, as well as NCI grant P41CA196276 for financial support of this work. H.L.T. was supported by NIH R21 AI111662. S.K.E. thanks the NSF GRFP (DGE 1650113) for financial support. F.D.T. thanks Novartis Institutes for Biomedical Research and the Novartis-Berkeley Center for Proteomics and Chemistry Technologies for supporting this work. A.H.C. thanks the NSF Graduate Research Fellowship Program (Division of Graduate Education 1106400) for financial support. C.J.C. acknowledges the NIH (ES4705 and ES28096) and the Aduro-Berkeley Immunotherapeutics and Vaccine Research Initiative program for financial support. C.J.C. is an Investigator with the Howard Hughes Medical Institute and a Canadian Institute for Advanced Research Senior Fellow.

1. C. D. Spicer, B. G. Davis, Selective chemical protein modification. *Nat. Commun.* **5**, 4740 (2014).
2. S. Lin *et al.*, Redox-based reagents for chemoselective methionine bioconjugation. *Science* **602**, 597–602 (2017).
3. K. F. Dyer, The quiet revolution: A new synthesis of biological knowledge. *J. Biol. Educ.* **5**, 15–24 (1971).
4. G. P. Adams, L. M. Weiner, Monoclonal antibody therapy of cancer. *Nat. Biotechnol.* **23**, 1147–1157 (2005).
5. Y. Mao, J. M. Mullins, Conjugation of fluorochromes to antibodies. *Methods Mol. Biol.* **588**, 43–48 (2010).
6. C. F. Meares *et al.*, Conjugation of antibodies with bifunctional chelating agents: Isothiocyanate and bromoacetamide reagents, methods of analysis, and subsequent addition of metal ions. *Anal. Biochem.* **142**, 68–78 (1984).
7. S. Darmanis *et al.*, Simultaneous multiplexed measurement of RNA and proteins in single cells. *Cell Rep.* **14**, 380–389 (2016).
8. M. Stoeckius *et al.*, Simultaneous epitope and transcriptome measurement in single cells. *Nat. Methods* **14**, 865–868 (2017).
9. J. Tushir-Singh, Antibody-siRNA conjugates: Drugging the undruggable for anti-leukemic therapy. *Expert Opin. Biol. Ther.* **17**, 325–338 (2017).
10. J. F. DiJoseph *et al.*, Antibody-targeted chemotherapy with CMC-544: A CD22-targeted immunocjugate of calicheamicin for the treatment of B-lymphoid malignancies. *Blood* **103**, 1807–1814 (2004).
11. P. C. Egan, J. L. Reagan, The return of gemtuzumab ozogamicin: A humanized anti-CD33 monoclonal antibody-drug conjugate for the treatment of newly diagnosed acute myeloid leukemia. *Oncotargets Ther.* **11**, 8265–8272 (2018).
12. G. D. L. Phillips *et al.*, Targeting HER2-positive breast cancer with trastuzumab-DM1, an antibody-cytotoxic drug conjugate. *Canc. Res.* **68**, 9280–9290 (2008).
13. A. Younes *et al.*, Brentuximab vedotin (SGN-35) for relapsed CD30-positive lymphomas. *N. Engl. J. Med.* **363**, 1812–1821 (2010).
14. A. Beck, L. Goetsch, C. Dumontet, N. Corvaia, Strategies and challenges for the next generation of antibody-drug conjugates. *Nat. Rev. Drug Discov.* **16**, 315–337 (2017).
15. C. Chalouni, S. Doll, Fate of antibody-drug conjugates in cancer cells. *J. Exp. Clin. Oncol.* **37**, 1–12 (2018).
16. S. Panowski, S. Bhakta, H. Raab, P. Polakis, J. R. Junutula, Site-specific antibody drug conjugates for cancer therapy. *mAbs* **6**, 34–45 (2014).
17. K. Tsuchikama, Z. An, Antibody-drug conjugates: Recent advances in conjugation and linker chemistries. *Protein Cell* **9**, 33–46 (2018).
18. K. J. Hamblett *et al.*, Effects of drug loading on the antitumor activity of a monoclonal antibody drug conjugate. *Clin. Canc. Res.* **10**, 7063–7070 (2013).
19. P. Bryant *et al.*, In vitro and in vivo evaluation of cysteine rebridged trastuzumab-MMAE antibody drug conjugates with defined drug-to-antibody ratios. *Mol. Pharm.* **12**, 1872–1879 (2015).
20. L. P. Y. Liu-Shin, A. Fung, A. Malhotra, G. Ratnaswamy, Evidence of disulfide bond scrambling during production of an antibody-drug conjugate. *mAbs* **10**, 1190–1199 (2018).
21. J. R. Junutula *et al.*, Site-specific conjugation of a cytotoxic drug to an antibody improves the therapeutic index. *Nat. Biotechnol.* **26**, 925–932 (2008).
22. R. Ohri *et al.*, High-throughput cysteine scanning to identify stable antibody conjugation sites for maleimide- and disulfide-based linkers. *Bioconjugate Chem.* **29**, 473–485 (2018).
23. H. Persson *et al.*, CDR-H3 diversity is not required for antigen recognition by synthetic antibodies. *J. Mol. Biol.* **425**, 803–811 (2013).
24. M. Hornsby *et al.*, A high through-put platform for recombinant antibodies to folded proteins. *Mol. Cell. Proteomics* **14**, 2833–2847 (2015).
25. A. H. Christian *et al.*, A physical organic approach to tuning reagents for selective and stable methionine bioconjugation. *J. Am. Chem. Soc.* **141**, 12657–12662 (2019).
26. B. A. Mendelsohn *et al.*, Investigation of hydrophilic auristatin derivatives for use in antibody drug conjugates. *Bioconjugate Chem.* **28**, 371–381 (2017).
27. X. Gao *et al.*, Effect of individual Fc methionine oxidation on FcRn binding: Met252 oxidation impairs FcRn binding more profoundly than Met428 oxidation. *J. Pharmaceut. Sci.* **104**, 368–77 (2015).
28. M. Habberger *et al.*, Assessment of chemical modifications of sites in the CDRs of recombinant antibodies: Susceptibility vs. functionality of critical quality attributes. *mAbs* **6**, 327–339 (2014).
29. T. T. Kuo, V. G. Aveson, Neonatal Fc receptor and IgG-based therapeutics. *mAbs* **3**, 422–430 (2011).
30. S. Y. Pyun, T. R. Kim, C. R. Lee, W. G. Kim, Kinetics studies on the mechanism of hydrolysis of S-phenyl-S-vinyl-N-p-tosylsulfonamide derivatives. *Bull. Kor. Chem. Soc.* **24**, 306–310 (2003).
31. B. Q. Shen *et al.*, Conjugation site modulates the in vivo stability and therapeutic activity of antibody-drug conjugates. *Nat. Biotechnol.* **30**, 184–189 (2012).
32. M. T. Taylor, J. E. Nelson, M. G. Suero, M. J. Gaunt, A protein functionalization platform based on selective reactions at methionine residues. *Nature* **562**, 563–568 (2018).
33. C. Eigenbrot, M. Randal, L. Presta, P. Carter, A. A. Kossiakoff, X-ray structures of the antigen-binding domains from three variants of humanized anti-p185HER2 antibody 4D5 and comparison with molecular modeling. *J. Mol. Biol.* **229**, 969–995 (1993).
34. B. Webb, A. Sali, Comparative protein structure modeling using MODELLER. *Curr. Protoc. Bioinformatics* **2016**, 1–5 (2016).
35. I. Sassoon, V. Blanc, Antibody-drug conjugate (ADC) clinical pipeline: A review. *Methods Mol. Biol.* **1045**, 1–27 (2013).